Author Manuscript

Author Manuscript

Author Manuscript

Author Manuscript

HHS Public Access

Author manuscript

Pain. Author manuscript; available in PMC 2016 May 01.

Published in final edited form as:

Pain. 2015 May ; 156(5): 825–836. doi:10.1097/j.pain.0000000000000120.

Reactive oxygen species (ROS) mediate visceral pain-related amygdala plasticity and behaviors

Guangchen Ji[a], **Zhen Li**[b], and **Volker Neugebauer**[a]

[a]Department of Pharmacology and Neuroscience, Texas Tech University Health Sciences Center (TTUHSC), School of Medicine, 3601 4th Street, Mail Stop 6592, Lubbock, Texas 79430-6592

[b]Institute for Biomedical Sciences of Pain & Institute for Functional Brain Disorders, The Fourth Military Medical University, 1 Xinsi Road, Xi'an 710038, P.R. China, Phone: +86-29-84778642, FAX: +86-29-84777945

Introduction

Clinical and pre-clinical evidence has established the amygdala as an important player in the emotional-affective dimension of pain [3;56;58;69]. In humans, increased amygdala activity is seen in experimental and clinical pain conditions, including visceral pain [4;39;40;45;69;72]. The amygdala is a limbic brain area in the medial temporal lobe and consists of several subnuclei. The amygdala circuitry that contributes to the emotional-affective component of pain is centered on the lateral-basolateral (LA-BLA) and central (CeA) nuclei [56;58]. The CeA serves output functions and receives nociceptive-specific input from the parabrachial area whereas the LA-BLA network provides highly processed nociceptive and affect-related information to the CeA. Neuroplasticity in the LA-BLA-CeA network correlates positively with pain behaviors in animals, and interventions that deactivate the amygdala have inhibitory effects in different pain models (for recent reviews see [3;56]), including visceral pain [13;24;31;71]. Still, little is known about synaptic and cellular mechanisms of viscero-nociceptive processing in the amygdala.

Reactive oxygen species (ROS), such as superoxide and hydrogen peroxide, play an important role in physiological plasticity critical for cognitive processes such as memory, but abnormally increased ROS levels have detrimental effects [49;51;61] and are involved in pain pathophysiology [11]. Inhibition of ROS production with ROS scavengers administered peripherally [33;74] or spinally [18;35;36;67;68;75] has antinociceptive effects in models of inflammatory and neuropathic pain. While evidence for an important role of peripheral and spinal ROS in pain mechanisms is accumulating, pain-related functions of ROS in the brain remain to be determined.

Recent work from our laboratory showed that under normal conditions ROS scavengers in the amygdala inhibit visceral and somatosensory nociceptive responses [29] and excitability

Corresponding author: Volker Neugebauer, M.D, Ph.D., Professor and Chair, Department of Pharmacology and Neuroscience, Texas Tech University Health Sciences Center | School of Medicine, 3601 4th Street | Mail Stop 6592, Lubbock, Texas 79430-6592, Phone: (806) 743-3880, volker.neugebauer@ttuhsc.edu.

There are no conflicts of interest.

Author Manuscript Author Manuscript Author Manuscript Author Manuscript

[44] of CeA neurons induced by the activation of metabotropic glutamate receptors. However, the role of endogenous ROS in pain-related changes in the amygdala is not yet known. Here we tested the effect of a membrane-permeable ROS scavenger, the superoxide dismutase mimetic tempol [34;43], to examine the contribution of ROS to pain behaviors, nociceptive processing and synaptic transmission in a rat model of visceral pain induced by intracolonic zymosan. The behavioral and electrophysiological analysis of the effects of a ROS scavenger in the amygdala in a pain model is a key novelty of this study.

Methods

Male Sprague Dawley rats (250–350 g for in vivo assays and 150–220 g for brain slice studies) were housed in a temperature controlled room and maintained on a 12 h day/night cycle. Water and food were available ad libitum. All experimental procedures were approved by the Institutional Animal Care and Use Committees (IACUC) at the University of Texas Medical Branch (UTMB), where some of the experiments were carried out, and at Texas Tech University Health Sciences Center (TTUHSC), where the studies were finalized, and conform to the guidelines of the International Association for the Study of Pain (IASP) and of the National Institutes of Health (NIH).

Visceral pain model

Zymosan (1 ml, 25 mg/ml in saline) was injected into the descending colon (7 cm from the anus) using a polyethylene tube attached to a syringe. The time point of 4–5 h postinjection was selected to study visceral pain-related behavioral and electrophysiological changes. Within a few hours intracolonic zymosan produces colorectal hypersensitivity and an initial monocyte-based inflammation (colitis) lasting for about 24 h [15]. Control animals included normal untreated rats as well as sham rats that received intracolonic sterile saline instead of zymosan. In some experiments the same animal was studied before and after zymosan injection. Experimental protocols for the different behavioral and electrophysiological assays are described in Methods and Results.

Behavioral studies

Vocalizations—Vocalizations in the audible (20 Hz to 16 kHz) and ultrasonic (25 ± 4 kHz) ranges were recorded and analyzed as described previously [23;27;50;63]. The experimental setup (U.S. Patent 7,213,538) included a custom-designed recording chamber, a condenser microphone connected to a preamplifier, an ultrasound detector, filter and amplifier (UltraVox four-channel system; Noldus Information Technology), and data acquisition software (UltraVox 2.0; Noldus Information Technology). The computerized recording system detected the occurrence of vocalizations within user-defined frequencies. Animals were placed in the recording chamber for acclimation 1 h before the vocalization measurements. Vocalizations were measured during brief (10 s) colorectal distension (CRD) with innocuous (20 mmHg) and noxious (80 mmHg) intraluminal pressure. For CRD an inflatable latex balloon (5 cm) connected to a sphygmomanometer was inserted into the distal colon at the beginning of the acclimation period [29;44]. The total duration of vocalizations (arithmetic sum of the duration of individual events) was recorded for 1 min, starting with the onset of the visceral stimulus. Audible and ultrasonic vocalizations reflect

Author Manuscript Author Manuscript Author Manuscript Author Manuscript

supraspinally organized nocifensive and affective responses to aversive stimuli [57]. Vocalization measurements were made in the same animals before and after induction of the visceral pain model (4–5 h and, in some cases, 10 h; paired paradigm).

Elevated plus-maze (EPM) test—Anxiety-like behavior was measured in the elevated plus-maze (Columbus Instruments) as described previously [50;63]. The EPM had two closed and two open arms arranged in a plus shape. The platform was elevated 70 cm above the floor. The EPM was equipped with photocells to detect animal movements in the open and closed arms using Multi-Varimex software (Columbus Instruments). Disruption of a photobeam by the rat was registered as entry into the respective arm. The animal was placed on the central area of the EPM, facing an open-arm. Anxiety-like behavior was measured as the ratio of open-arm entries to the total number of entries (expressed as %) during 5 min. Total number of entries was calculated as the arithmetic sum of open-arm entries and closed-arm entries. The test was done in sham controls (intracolonic saline) and zymosan-injected rats (unpaired paradigm). Each animal was tested only once in the EPM.

Conditioned place preference (CPP)—The test apparatus (Columbus Instr.) consisted of two chambers (30×30×40 cm each) with distinguishing features (wall color, floor texture), a neutral zone, and a computerized analysis system that measured the movements of the animal between the chambers, movements within each chamber and time spent in each chamber. The experimental protocol was similar to that described by King et al. [37]. After pre-conditioning baseline measurements (3 days; to show a lack of chamber preference) rats received vehicle paired with one chamber as control, and drug treatment (tempol; see “Drugs”) paired with the opposite chamber 4 h later (conditioning phase). Rats were confined for 30 min to the appropriate chamber 15 min after drug administration based on the time course of drug effects determined in the electrophysiology studies. Chamber pairings were counterbalanced. On test day, 20 h after drug pairing, rats were placed in the CPP box with access to both chambers and behavior was recorded for 15 min to analyze chamber preference based on time spent in each chamber. Measurements were made in sham controls (intracolonic saline) and in rats with intracolonic zymosan (unpaired paradigm).

Drug application by microdialysis—As described in detail previously [27;50;57;63], a guide cannula was implanted stereotaxically the day before behavioral measurements while the animal was anesthetized with pentobarbital sodium (Nembutal; 50 mg/kg, i.p.). The guide cannula was implanted on the dorsal margin of the CeA in the right hemisphere using the following coordinates (in mm): 2.3 caudal to bregma; 4.0 lateral to midline; depth, 7.0. In some experiments a guide cannula was implanted into the striatum as a placement control (2.3 caudal to bregma; 4.2 lateral to midline; depth of tip, 5.5). The cannula was fixed to the skull with dental acrylic (Plastics One). Antibiotic ointment was applied to the exposed tissue to prevent infection. On the day of the experiment, a microdialysis probe (CMA11; CMA/Microdialysis; membrane diameter, 250 μm; membrane length, 1 mm; 8 kDa cutoff) was inserted through the guide cannula so that the probe protruded by 1 mm. The probe was perfused with artificial cerebrospinal fluid (ACSF) containing the following (in mM): 125.0 NaCl, 2.6 KCl, 2.5 NaH_2PO_4, 1.3 $CaCl_2$, 0.9 $MgCl_2$, 21.0 $NaHCO_3$, and 3.5 glucose;

Author Manuscript Author Manuscript Author Manuscript Author Manuscript

oxygenated and equilibrated to pH 7.4 at 5 μl/min. Before each drug application, ACSF was pumped through the fiber for at least 1 h to establish equilibrium in the tissue.

Drugs—4-hydroxy-2,2,6,6-tetramethylpiperidine-N-oxyl (tempol, membrane-permeable ROS scavenger, superoxide dismutase mimetic; purchased from Tocris Bioscience) [34;43] was used in this study. Tempol was dissolved in water for stock solutions and diluted in ACSF to the final concentration on the day of the experiment (100-fold that predicted to be needed based on data from our previous studies [29;44]). Drug concentration in the tissue is at least 100 times lower than in the microdialysis probe as a result of the concentration gradient across the dialysis membrane and diffusion in the tissue. Numbers in the text refer to drug concentrations in the microdialysis fiber.

Histology—The position of the microdialysis probes in the amygdala was verified histologically as in our previous studies [29;44;63].

Electrophysiology in anesthetized rats

Extracellular single-unit recordings were made from CeA neurons (capsular division) in rats anesthetized with pentobarbital as described before [27;29;50]. Individual neurons were recorded in sham control rats (intracolonic saline) and in another group of rats before and after intra-colonic zymosan injection (visceral pain model).

Animal preparation and anesthesia—The animal was anesthetized with pentobarbital sodium (induction, 50 mg/kg, i.p.; maintenance, 15 mg/kg per h, i.v.). After paralysis with pancuronium (0.3 mg/h, i.v.) the animal was artificially ventilated (3–3.5 ml; 55–65 strokes/min). Physiological parameters such as end-tidal CO_2 levels (kept at 4.0 %), heart rate and core body temperature (kept at 37 °C) were continuously monitored. The animal was mounted in a stereotaxic frame (David Kopf Instr.). A small unilateral craniotomy at the sutura fronto-parietalis level allowed the insertion of the recording electrode and microdialysis probe.

Electrophysiological recording and identification of CeA neurons—Extracellular single-unit recordings of CeA neurons were made with glass insulated carbon filament electrodes (4 – 6 MΩ), using the following stereotaxic coordinates [59]: 2.2–3.1 caudal to bregma, 3.8–4.2 lateral to midline, depth 6.5–8.0. Recorded signals were amplified, band-pass filtered (300 Hz – 3 kHz), displayed on an analog oscilloscope, fed into a window discriminator (World Precision Instruments), digitized (1401 Plus interface, Cambridge Electronic Design, CED), and recorded on a personal computer (PC) using Spike2 software (CED version 4) for spike sorting, data storage, and analysis of single-unit activity. Spike size and configuration were continuously monitored. Only those neurons were included in the study whose spike configuration matched a pre-set template and could be clearly discriminated from activity in the background.

Experimental protocol—In each animal, background and evoked activity of only one neuron were recorded as described in detail previously [29;30;50]. An individual CeA neuron was identified by its background activity and responses to brief search stimuli, which

Author Manuscript Author Manuscript Author Manuscript Author Manuscript

included compression of skin folds and deep tissue (joint and muscles). Visceral stimuli (colorectal distension, CRD; see "Behavioral studies") were used sparingly to identify neurons with visceral input. Our previous work showed that the vast majority (>95%) of viscero-nociceptive amygdala neurons also respond to somatosensory mechanical stimuli [29]. In each experiment one CeA neuron that responded to CRD was selected for pharmacological studies. Background activity in the absence of any intentional stimulation was recorded for 10 min. Brief (10 s) CRDs with different intensities (innocuous, 20; moderate, 40; noxious, 60 and 80 mmHg) were tested before and during drug application. For the analysis of net evoked activity, background activity in the 10 s time period preceding the 10 s stimulus was subtracted from the total activity during stimulation. Drug effects on CeA neurons were tested in sham control rats and in rats with intracolonic zymosan (4–5 h postinjection; in these animals the neurons were recorded before and after injection but drugs were tested only after zymosan).

Drugs and drug application—A microdialysis probe (CMA11; CMA/Microdialysis) was inserted stereotaxically into the amygdala (CeA) through the craniotomy (see previous section) at least 1 hour before the recordings started. The probe was connected to an infusion pump (Harvard Apparatus). ACSF (composition see "Behavioral studies") was present in the probe throughout the experiment and served as vehicle control. Tempol (see "Behavioral studies") was administered by microdialysis at a rate of 5 μl/min.

Histology—Recording sites and position of the microdialysis probes in the amygdala were verified histologically as in our previous studies [29;44;63].

Electrophysiology in brain slices

Whole-cell patch-clamp recordings of neurons in the CeA (capsular division) were made in brain slices from sham controls (intracolonic saline) and from rats with intracolonic zymosan (5 h postinduction).

Slice preparation—Coronal brain slices (300–500 μm) containing the CeA were obtained as previously described (for recent references see [44;63]). Rats were decapitated without the use of anesthesia to avoid chemical contamination of the tissue. A single brain slice was transferred to the recording chamber and submerged in ACSF (31 °C), which superfused the slice at ~2 ml/min. ACSF contained (in mM) NaCl 117, KCl 4.7, NaH_2PO_4 1.2, $CaCl_2$ 2.5, $MgCl_2$ 1.2, $NaHCO_3$ 25, and glucose 11; oxygenated and equilibrated to pH 7.4 with a mixture of 95% O_2/5% CO_2. Only one or two brain slices per animal were used. Only one neuron was recorded in each slice and a fresh slice was used for each new experimental protocol. Numbers in the manuscript refer to the number of neurons.

Patch-clamp recording—Whole-cell current- and voltage-clamp recordings were made from CeA neurons using the "blind" patch technique or DIC-IR video-microscopy as described before (for recent references see [44;63]). The boundaries of the different amygdalar nuclei are easily seen under light microscopy (see Fig. 1 in [17] and Fig. 9 in [63]). Recording pipettes (3–5 MΩ tip resistance) made from borosilicate glass (1.5 mm and 1.12 mm, outer and inner diameter, respectively; Drummond) were filled with intracellular

Author Manuscript Author Manuscript Author Manuscript Author Manuscript

solution containing (in mM): 122 K-gluconate, 5 NaCl, 0.3 $CaCl_2$, 2 $MgCl_2$, 1 EGTA, 10 HEPES, 5 Na_2-ATP, and 0.4 Na_3-GTP; pH was adjusted to 7.2–7.3 with KOH and osmolarity to 280 mOsm/kg with sucrose. For data acquisition and analysis a dual four-pole Bessel filter (Warner Instr.), low-noise Digidata 1322 interface (Axon Instr.), Axoclamp-2B amplifier (Axon Instr.), Pentium PC, and pClamp9 software (Axon Instr.) were used. Signals were low-pass filtered at 1 kHz and digitized at 5 kHz. Head-stage voltage was monitored continuously on an oscilloscope to ensure precise performance of the amplifier. High (> 2 GΩ) seal and low (< 20 MΩ) series resistances were checked throughout the experiment (using pClamp9 membrane test function) to ensure high-quality recordings. If series resistance (monitored with pClamp9 software) changed more than 10%, the neuron was discarded.

Neuronal excitability—Frequency-current [F-I] relationships were measured in current-clamp mode by recording action potentials generated by intracellular current injections (500 ms) of increasing magnitude while the neuron was held at a starting membrane potential of −60 mV (see [44]).

Synaptic transmission—Neurons were voltage-clamped at −60 mV for the recording of excitatory postsynaptic currents (EPSCs). EPSCs were pharmacologically isolated with bicuculline (30 μM) and could be blocked with NBQX (10 μM). Using concentric bipolar stimulating electrodes (SNE-100, David Kopf Instruments), EPSCs were evoked by focal electrical stimulation (150 μs square-wave pulses) of axons presumably from the parabrachial area (PB) at a frequency of 0.033 Hz. The stimulation electrode was positioned on the afferent fiber tract from the lateral PB, which runs dorsomedial to the CeA and ventral to but outside of the caudate-putamen [17;44;63] (see Discussion). Input–output relationships of evoked EPSCs were obtained by increasing the stimulus intensity in 100 μA steps. For evaluation of a drug effect on synaptically evoked responses, the stimulus intensity was set to 50% of the intensity required for maximum responses. Peak amplitudes of individual EPSCs were measured and averaged. Evoked synaptic transmission was measured every 3–5 min before and during drug application. Miniature EPSCs (in 1 μM TTX) were recorded at −70 mV as described before [63;64]. A fixed length of traces (5 min) was analyzed for frequency and amplitude distributions using MiniAnalysis program 5.3 (Synaptosoft). The root mean square (RMS) of background noise was computed for each set of data. Detection threshold was set to 3–4 times the RMS value. Peaks were detected automatically, but each detected event was then visually inspected to prevent the inclusion of false data. Miniature EPSCs were measured 5–10 min before and 10–15 min during drug application.

Drug application—Drugs were applied by gravity-driven superfusion of the brain slice in the ACSF (~2 ml/min). Solution flow into the recording chamber (1 ml volume) was controlled with a three-way stopcock.

Statistical analysis

All averaged values are given as the mean ± standard error of the mean (SEM). GraphPad Prism 3.0 software (Graph-Pad, San Diego, CA) was used for all statistical analyses except

Author Manuscript Author Manuscript Author Manuscript Author Manuscript

for cumulative distribution analysis of miniature synaptic events in the patch-clamp studies where the Kolmogorov-Smirnov test was used (MiniAnalysis program 5.3, Synaptosoft Inc.). Statistical analysis was performed on the raw data. Student's paired *t*-test was used to compare 2 sets of data. For multiple comparisons, repeated-measures ANOVA, one-way ANOVA or two-way ANOVA were used with appropriate posttests as indicated in the text and figure legends. Parametric analyses were justified because Bartlett's tests for equal variances showed no significant differences. Statistical significance was accepted at the level $P < 0.05$.

Results

A ROS scavenger in the amygdala inhibits visceral pain-related behaviors

Vocalizations—Audible and ultrasonic vocalizations were evoked by brief (10 s) colorectal distension (CRD) with innocuous (20 mmHg) and noxious (80 mmHg) intraluminal pressure (see Methods). Vocalizations increased 4–5 h after intracolonic zymosan (colitis, visceral pain model; see Methods) significantly ($P < 0.05$-0.001, Bonferroni posttests following repeated-measures ANOVA; Fig. 1; n = 5 rats in A/B and n = 5 rats in C/D) and remained elevated for at least 10 h post-injection of zymosan when tested in n = 5 rats (data not shown). No vocalizations were detected in the absence of any intentional stimulation (CRD, 0 mmHg). Measurements were made in the same animals before and after induction of the visceral pain model. Stereotaxic application of a ROS scavenger (superoxide dismutase mimetic tempol, 100 mM, concentration in microdialysis probe) into the amygdala (CeA) had no effect on vocalizations of normal rats but inhibited the increased vocalizations of the same animals 5 h after intracolonic zymosan significantly ($P < 0.05$, Bonferroni posttests; Fig. 1A and B). Results of repeated-measures ANOVA were as follows. Audible vocalizations (Fig. 1A), $P < 0.001$, innocuous CRD, $F_{3,12} = 12.11$; noxious CRD, $F_{3,12} = 24.16$; ultrasonic vocalizations (Fig. 1B), $P < 0.001$, innocuous CRD, $F_{3,12} = 21.79$; noxious CRD, $F_{3,12} = 12.10$.

Off-site application of tempol into the adjacent striatum had no significant effect on vocalizations ($P > 0.05$, Bonferroni posttests, n = 5 rats; Fig. 1C and D). Results of repeated-measures ANOVA were as follows. Audible vocalizations (Fig. 1A), $P < 0.05$, innocuous CRD, $F_{2,8} = 6.43$; noxious CRD, $F_{2,8} = 5.99$; ultrasonic vocalizations (Fig. 1B), innocuous CRD, $P < 0.001$, $F_{2,8} = 21.79$; noxious CRD, $P < 0.01$, $F_{3,12} = 18.03$.

Drug effects were compared to predrug baseline vocalizations measured in the presence of ACSF (vehicle control; see Methods). Vocalizations were measured at 15 min after starting drug application because the electrophysiology studies detected effects of tempol at that time point (see Fig. 5B and time course in Fig. 7E). Drug applications were made in the right hemisphere because of previous evidence for pain-related lateralization [8;21;28] although it should be noted that lateralization in visceral pain remains to be determined. Position of microdialysis probes in the CeA or striatum was verified histologically (see Figs. 9 and 10).

Anxiety-like behavior—The ratio of open-arm entries to the total number of entries (expressed as %) in the elevated plus-maze was measured in sham controls and in rats with

Author Manuscript Author Manuscript Author Manuscript Author Manuscript

intracolonic zymosan (colitis, 5 h post-injection; Fig. 2A). Zymosan-injected rats received stereotaxic application of either ACSF (vehicle) or tempol (100 mM, concentration in microdialysis probe) into the amygdala (CeA) for 15 min immediately before they were placed in the EPM. Open-arm preference was significantly decreased in the visceral pain model ("colitis"; $P < 0.05$, Bonferroni posttest; $n = 5$ rats) compared to controls ($n = 5$). Tempol increased the open-arm preference of zymosan-injected rats significantly ($P < 0.05$, Bonferroni posttest; $n = 6$ rats), suggesting anxiolytic effects. To determine any effects of tempol on locomotor activity, the total number of entries into the open and closed arms of the EPM was measured for 5 min (Fig. 2B; same animals and test as in Fig. 2A). Zymosan-injected rats showed a decreased number of entries compared to controls ($P < 0.001$, Bonferroni posttest), but tempol had no significant effect on locomotor activity ($P > 0.05$). The data suggest that tempol can inhibit anxiety-like behavior without affecting locomotion.

Conditioned place preference (CPP)—The CPP test was performed in sham control rats ($n = 7$; Fig. 3A) and in rats with intracolonic zymosan ($n = 6$; Fig. 3B). After habituation to the two chambers of the CPP apparatus (see Methods) animals received stereotaxic application of ACSF (vehicle) into the CeA paired with one chamber and 4 h later stereotaxic application of tempol (100 mM, concentration in microdialysis probe) paired with the opposite chamber. Animals did not show a preference for one chamber before vehicle or drug pairing (pre-CPP). Tempol induced a place preference in the visceral pain model (colitis), i.e., rats preferred the chamber that was paired with tempol ($P < 0.001$, Bonferroni posttest; Fig. 3B), whereas sham control rats did not show any place preference (Fig. 3A). We interpret the data suggest that tempol relieved an aversive state in the visceral pain model but had no effect in the absence of pain under normal conditions.

A ROS scavenger inhibits visceral pain-related activity of amygdala neurons

Extracellular recordings were made from 12 CeA neurons (capsular division) in 12 anesthetized rats as described before [29;50]. Recordings were made in the right hemisphere because of previous evidence for pain-related lateralization [8;21;28]. Neurons were initially identified by their spontaneous activity and responses to brief mechanical search stimuli applied to skin and deep tissue (joints and muscles). CeA neurons had bilateral symmetrical receptive fields in the deep tissue and responded more strongly to noxious (1500 g/30 mm^2) than to innocuous (500 g/30 mm^2) stimuli (tissue compression) and were therefore classified as multireceptive neurons as in our previous studies. Next, brief (10 s) CRD was used to test for viscero-sensitivity. We identified 12 CeA neurons that were also activated by CRD (see individual example in Fig. 4A). Based on their graded responses to CRD of increasing intensities (20, 40, 60, and 80 mmHg) these neurons were classified as viscero-nociceptive neurons. CRD of 20 mmHg is considered innocuous, 40 mmHg is a moderate stimulus, whereas 60 and 80 mmHg are noxious stimulus intensities [2;29].

Seven of these 12 CeA neurons were recorded before and during the development of the zymosan-induced visceral pain state (colitis). Background activity and CRD-evoked responses of CeA neurons ($n = 7$) increased after intracolonic zymosan significantly ($P < 0.01$ and 0.001, compared to the activity of the same neurons before zymosan injection, Bonferroni posttests following repeated-measures ANOVA; Fig. 5B). An individual neuron

Author Manuscript Author Manuscript Author Manuscript Author Manuscript

is shown in Figure 4. Stereotaxic application of tempol (100 mM, concentration in microdialysis fiber) into the CeA decreased background activity and responses of these neurons (n = 7) to CRD in the visceral pain model significantly ($P < 0.05$-0.001 compared to predrug ACSF vehicle control, Bonferroni posttests; Fig. 5B). These neurons were recorded before and after intracolonic zymosan, but tempol was tested only in the visceral pain model (5 h postinjection). Background and evoked activity shown in Figure 5 was measured at 15 min after starting drug application, which is consistent with the time course of drug effects recorded in the ex vivo preparation (see Fig. 7E). Results of repeated-measures ANOVA were as follows (Fig. 5B). Background activity, $P < 0.001$, $F_{2,12} = 29.67$; innocuous CRD, $P < 0.001$, $F_{2,12} = 24.17$; noxious CRD, $P < 0.01$, $F_{2,12} = 9.62$.

Tempol had no effect on background and evoked activity in another set of CeA neurons recorded in sham control rats (3–5 h after intracolonic saline; n = 5, Fig. 5A). Note that responses in saline controls (Fig. 5A) were similar to the baseline responses in normal animals before colitis induction (Fig. 5B). Further, by the time tempol was tested in sham controls or in rats with colitis, animals had been under pentobarbital-anesthesia for about the same amount of time (8–9 h). Recording sites in the CeA were verified histologically (see Fig. 9). The data suggest that ROS are involved in the enhanced activity of amygdala neurons in a model of visceral pain.

A ROS scavenger inhibits excitability and excitatory synaptic transmission of CeA neurons in a visceral pain model

Neuronal excitability—As an established measure of neuronal excitability [44], frequency-current [F-I] relationships of neurons in the CeA (capsular division) were obtained using whole-cell current-clamp recordings of action potentials generated by intracellular injections of depolarizing current pulses (Fig. 6). Recordings were made in brain slices from sham controls and from rats with intracolonic zymosan (colitis, 5 h postinjection). Confirming the results of our previous study [24] we found increased neuronal excitability of CeA neurons in the visceral pain model (see predrug data in Fig. 6A and B), although we did not perform a statistical analysis here because the focus was on the role of ROS. Tempol (1 mM, 10–15 min) had no significant effect on CeA neurons in slices from sham controls (n = 5 neurons, $F_{1,56} = 5.42$, $P > 0.05$, main effect of drug, two-way ANOVA; Fig. 6A) but decreased input-output functions of neuronal excitability in brain slices from zymosan-injected rats significantly (n = 6 neurons, $F_{1,70} = 13.66$, $P < 0.001$, main effect of drug, two-way ANOVA; Fig. 6B).

Excitatory synaptic transmission—Input-output functions of monosynaptic EPSCs were measured in CeA neurons from sham controls and from rats with intracolonic zymosan (colitis, 5 h postinjection) using whole-cell voltage-clamp recordings (Fig. 7). Presumed inputs from the parabrachial area were stimulated as described previously by our group and others [17;32;44;54;63;76]. Consistent with our previous study [24] excitatory transmission was significantly increased in the visceral pain model (n = 13 neurons) compared to control transmission (n = 10 neurons; $F_{1,210} = 19.95$, $P < 0.001$, main effect of drug, two-way ANOVA; Fig. 7A). EPSCs were monosynaptic showing constant latency and kinetics and were blocked by a non-NMDA receptor antagonist (NBQX; Fig. 7B). Tempol (1 mM, 10–

Author Manuscript Author Manuscript Author Manuscript Author Manuscript

15 min) had no effect on baseline transmission in slices from sham controls (n = 5 neurons; Fig. 7C) but inhibited EPSCs in slices from rats with intracolonic zymosan significantly (n = 9 neurons; $P < 0.001$, Bonferroni posttest; Fig. 7D) and in a reversible manner (after 20 min of washout). Time course analysis showed that tempol had significant inhibitory effects in slices from rats with colitis (n = 5 neurons) compared to controls (n = 5 neurons; $P < 0.001$, $F_{1,136} = 70.79$, two-way ANOVA) starting at 10 min of drug application and recovering upon washout (Fig. 7E).

Quantal analysis of miniature EPSCs (mEPSCs, in the presence of TTX, 1 μM) showed that tempol (1 mM, 15 min) had no effect in slices from sham controls (n = 5 CeA neurons, Fig. 8A–C) but decreased amplitude (Fig. 8E) and frequency (Fig. 8F) of mEPSCs in slices from rats with intracolonic zymosan (colitis, 5 h postinjection) significantly (n = 6 CeA neurons; $P < 0.001$ and 0.01, respectively, paired t-tests). The effect on both frequency and amplitude of mEPSCs suggests a combined pre- and post-synaptic site of action.

Discussion

The study includes several novelties. Our data show for the first time that ROS contribute to changes in amygdala processing in a pain model and that ROS in the brain serves as a mechanism of visceral pain. ROS do so by increasing the excitatory drive of amygdala output neurons in the CeA, resulting in increased excitability and neuronal activity to generate spontaneous and evoked pain behaviors. The finding is significant because the amygdala has emerged as an important contributor to emotional-affective aspects of pain in preclinical and clinical studies [3;56;58;69].

The role of the amygdala in visceral pain is still not well understood. Accumulating evidence suggests that amygdala activity correlates positively with visceral pain. Pharmacological or optogenetic activation of the CeA in mice increased viscero-nocifensive responses to bladder distention, whereas deactivation of the CeA with pharmacological or genetic strategies reduced these responses [13]. Activation of the CeA in rats with corticosterone implants induced visceral hypersensitivity (responses to CRD) [22;52] and increased CRD-evoked signals in the amygdala in a neuroimaging study [31]. CRD but not restraint stress induced c-Fos protein expression in the CeA of naive animals [73]. In a visceral pain model induced by intraperitoneal injection of acetic acid, increased c-fos mRNA expression was found in the CeA [53]. Excitotoxic lesions of the CeA abolished the acetic acid-induced conditioned place aversion [71]. Our own studies showed that CeA neurons respond to visceral stimuli (CRD) [29] and develop synaptic plasticity in a visceral pain model (zymosan-induced colitis) [24]. Imaging studies in humans found abnormalities in amygdala activation in patients with irritable bowel syndrome (IBS) [7;55;77]. However, mechanisms of viscero-nociceptive amygdala processing and the link between neuronal activity and behavior in a visceral pain model remain to be determined.

We focused on ROS because of their emerging role in pain mechanisms and involvement in brain processes, including in the amygdala, that have been associated with nervous system disorders in animal models and in humans [9;12;47;48;51;62;78]. The contribution of ROS to brain mechanisms of pain is not known, and so our study takes an important step towards

Author Manuscript Author Manuscript Author Manuscript Author Manuscript

filling this knowledge gap. Peripheral and spinal ROS, such as superoxide and hydrogen peroxide, have been linked to inflammatory and neuropathic pain mechanisms. Increased hydrogen peroxide levels were found in inflamed tissue, and peripherally injected hydrogen peroxide induced hyperalgesia [33]. Increased levels of superoxide dismutase 2 (SOD2) were measured in the spinal cord in the capsaicin pain model [67;68]. Intrathecal ROS scavengers inhibited hyperalgesia in models of inflammatory [42;67;68] and neuropathic [36] pain. ROS scavengers such as tempol inhibited capsaicin-induced central sensitization [42] and C-fiber-induced LTP in spinal dorsal neurons [43].

Our data show that endogenous ROS are present at functional levels in the amygdala in a visceral pain model but not under normal conditions. The conclusion is based on the effects of tempol on behavioral and electrophysiological outcome measures. Tempol is a water-soluble, membrane-permeable, non-toxic small molecule that functions as a superoxide dismutase mimetic and scavenges intracellular superoxide [5;10;38;41;46;70]. Detoxifying enzymes such as superoxide dismutases (SOD) normally control cellular levels of ROS [26]. Importantly, behavioral and electrophysiological effects of tempol were only detected in the visceral pain model but not under normal conditions, suggesting a change in functional levels of ROS in the pain model that could result from impaired SOD function. The fact that the effects of tempol were reversible (see Fig. 7) suggests that ROS drives amygdala processing without causing cytotoxic damage and would be consistent with impaired endogenous ROS control mechanisms. Pain-related mechanisms of ROS activation and downstream targets of ROS in amygdala neurons remain to be determined. Under control conditions exogenous activation of metabotropic glutamate receptor subtype 5 (mGluR5) can generate ROS to activate protein kinase A and ERK [29;44]. PKA and ERK can increase NMDA receptor function in the amygdala, contributing to pain-related synaptic plasticity [6;16]. However, there is no evidence to date that the spontaneously released amount of glutamate in the absence of evoked afferent input in slices from rats with visceral pain remains high enough to activate mGluRs to a level sufficient for maintained ROS production after isolation.

The lack of effect of tempol under normal conditions and in sham controls is unlikely due to insufficient drug concentrations, because the same concentration was effective in the colitis model in this study and inhibited ROS activation by metabotropic glutamate receptors in our previous studies in normal animals [29;44]. For stereotaxic drug application in the behavioral assays we used acute implantation in this and our previous studies to minimize the risk of losing animals due to dislocation of the guide cannulas and other factors. Tempol had no effect on vocalizations in the same animal before colitis but was inhibitory after colitis induction and had no effect on the EPM and CPP in sham controls but in rats with colitis subjected to the same surgical procedure. This pattern of effects would argue against a cofounding effect of the surgery. Testing tempol twice in some animals (Fig. 1A,B) may raise concerns about confounding effects, but these animals nevertheless developed increased responses in the subsequently induced colitis model just like animals that were not tested with tempol before colitis induction (Fig. 1C,D). Further, these increased responses were sensitive to tempol and tempol had no effect under control conditions. This pattern of changes and tempol effects argues against confounding effects of the experimental protocol.

Author Manuscript Author Manuscript Author Manuscript Author Manuscript

Target concentrations of tempol in the tissue and microdialysis probe were selected from the literature [34;41;43] and our own previous studies [29;44] that correlated in vivo and ex vivo effects of tempol and showed that a 100-fold higher concentration was needed in the microdialysis probe to achieve appropriate tissue concentrations. Through an action in the CeA, tempol inhibited higher integrated affective behaviors (vocalizations) while increasing open-arm choice in the EPM test (anxiolytic-like effect) and inducing place-preference in the CPP test (anti-aversive effect). This pattern of inhibiting and activating behaviors, which reflects an overall beneficial effect on affective pain aspects, argues against non-selective generalized behavioral inhibition. Tempol inhibited activity of CeA neurons at the systems level (anesthetized animal) and decreased excitatory drive and neuronal activity of CeA neurons in the reduced slice preparation, suggesting that functional ROS, particularly superoxide, are present locally in the amygdala circuitry that triggers and modulates pain behaviors. It should be noted that the brain slice is a reduced preparation with a well control environment devoid of exposure to anesthetics, the anesthetized preparation provides intact connectivity and constant CO_2 levels maintained through artificial ventilation, and the behavioral approach in awake animals is not confounded by anesthetics but relies on endogenous homeostatic controls systems. The similarities of tempol effects in these three distinct preparations would argue against fundamental differences in ROS function in the amygdala assessed in vivo and ex vivo.

Placement controls showed no effect of tempol in the striatum adjacent to the CeA, supporting a regional action in circuits relevant to pain-related behaviors. Our patch-clamp analysis in brain slices found inhibitory effects of tempol on excitatory transmission to CeA neurons in the capsular division that we and others identified as a cluster of “nociceptive” neurons [8;19;54;56;58]. As in previous studies from our laboratory [17;63] and others [54;76] the stimulation electrode was positioned on visually identified fibers dorsomedial to the CeA and ventral to but outside of the caudate-putamen. No afferents to the CeA other than from the lateral parabrachial area have been identified in the vicinity of this tract [14;25;66]. Nociceptive capsular CeA neurons are characterized by nociceptive-specific inputs from the spino-parabrachio-amygdala pain pathway [20]. While animals of different age groups were used in the in vivo and ex vivo studies, the same neuronal population was likely studied in both preparations for the following reasons: location of the neurons in the capsular CeA in the in vivo and patch-clamp experiments, activation by noxious stimuli in vivo and by synaptic inputs from the parabrachial area in brain slices, and similar pattern of effects of tempol seen with both experimental approaches.

Analysis of frequency and amplitude distribution of miniature EPSCs suggests that tempol acted pre- and post-synaptically to inhibit transmission and excitability. In the hippocampus, exogenously applied ROS (hydrogen peroxide) also had both pre- and post-synaptic effects but inhibited synaptic transmission and excitability [60]. ROS (hydrogen peroxide) inhibited dopamine release in the striatum [65] whereas only postsynaptic actions were detected at cortico-striatal synapses in aging [1]. Different forms of ROS may play unique roles at different synapses and in different models.

In conclusion, this study provides evidence for abnormal ROS function in a visceral pain model, resulting in enhanced drive and increased excitability of amygdala output neurons in

Author Manuscript Author Manuscript Author Manuscript Author Manuscript

the CeA. Scavenging ROS appears to present an opportunity to normalize brain functions and control amygdala-dependent emotional-affective behaviors associated with (visceral) pain.

Acknowledgments

This work was supported by National Institute of Neurological Disorders and Stroke (NIH/NINDS) Grants NS081121, NS038261 and NS011255. We thank Janet Dertien, Dept. of Pharmacology and Neuroscience at TTUHSC, for her excellent assistance with the histology.

Reference List

1. Akopian G, Walsh JP. Pre- and postsynaptic contributions to age-related alterations in corticostriatal synaptic plasticity. Synapse. 2006; 60:223–238. [PubMed: 16739119]
2. Al-Chaer ED, Lawand NB, Westlund KN, Willis WD. Visceral nociceptive input into the ventral posterolateral nucleus of the thalamus: a new function for the dorsal column pathway. J Neurophysiol. 1996; 76:2661–2674. [PubMed: 8899636]
3. Apkarian AV, Neugebauer V, Koob G, Edwards S, Levine JD, Ferrari L, Egli M, Regunathan S. Neural mechanisms of pain and alcohol dependence. Pharmacol Biochem Behav. 2013; 112C:34–41. [PubMed: 24095683]
4. Baliki MN, Geha PY, Jabakhanji R, Harden N, Schnitzer TJ, Apkarian AV. A preliminary fMRI study of analgesic treatment in chronic back pain and knee osteoarthritis. Mol Pain. 2008; 4:47. [PubMed: 18950528]
5. Bindokas VP, Jordan J, Lee CC, Miller RJ. Superoxide production in rat hippocampal neurons: selective imaging with hydroethidine. J Neurosci. 1996; 16:1324–1336. [PubMed: 8778284]
6. Bird GC, Lash LL, Han JS, Zou X, Willis WD, Neugebauer V. Protein kinase A-dependent enhanced NMDA receptor function in pain-related synaptic plasticity in rat amygdala neurones. J Physiol. 2005; 564:907–921. [PubMed: 15760935]
7. Bonaz B, Baciu M, Papillon E, Bost R, Gueddah N, Le Bas JF, Fournet J, Segebarth C. Central processing of rectal pain in patients with irritable bowel syndrome: an fMRI study. Am J Gastroenterol. 2002; 97:654–661. [PubMed: 11926209]
8. Carrasquillo Y, Gereau RW. Hemispheric lateralization of a molecular signal for pain modulation in the amygdala. Mol Pain. 2008; 4:24. [PubMed: 18573207]
9. Ceretta LB, Reus GZ, Abelaira HM, Ribeiro KF, Zappellini G, Felisbino FF, Steckert AV, Dal-Pizzol F, Quevedo J. Increased oxidative stress and imbalance in antioxidant enzymes in the brains of alloxan-induced diabetic rats. Exp Diabetes Res. 2012; 2012:302682. [PubMed: 22645603]
10. Chinopoulos C, Adam-Vizi V. Calcium, mitochondria and oxidative stress in neuronal pathology. Novel aspects of an enduring theme. FEBS J. 2006; 273:433–450. [PubMed: 16420469]
11. Chung JM. The Role of Reactive Oxygen Species (ROS) in Persistent Pain. Mol Interv. 2004; 4:248–250. [PubMed: 15471906]
12. Crema L, Schlabitz M, Tagliari B, Cunha A, Simao F, Krolow R, Pettenuzzo L, Salbego C, Vendite D, Wyse AT, Dalmaz C. Na+, K+ ATPase activity is reduced in amygdala of rats with chronic stress-induced anxiety-like behavior. Neurochem Res. 2010; 35:1787–1795. [PubMed: 20717721]
13. Crock LW, Kolber BJ, Morgan CD, Sadler KE, Vogt SK, Bruchas MR, Gereau RW. Central amygdala metabotropic glutamate receptor 5 in the modulation of visceral pain. J Neurosci. 2012; 32:14217–14226. [PubMed: 23055491]
14. Dobolyi A, Irwin S, Makara G, Usdin TB, Palkovits M. Calcitonin gene-related peptide-containing pathways in the rat forebrain. J Comp Neurol. 2005; 489:92–119. [PubMed: 15977170]
15. Feng B, La JH, Schwartz ES, Tanaka T, McMurray TP, Gebhart GF. Long-term sensitization of mechanosensitive and -insensitive afferents in mice with persistent colorectal hypersensitivity. Am J Physiol Gastrointest Liver Physiol. 2012; 302:G676–G683. [PubMed: 22268098]

Author Manuscript Author Manuscript Author Manuscript Author Manuscript

16. Fu Y, Han J, Ishola T, Scerbo M, Adwanikar H, Ramsey C, Neugebauer V. PKA and ERK, but not PKC, in the amygdala contribute to pain-related synaptic plasticity and behavior. Mol Pain. 2008; 4:26–46. [PubMed: 18631385]
17. Fu Y, Neugebauer V. Differential mechanisms of CRF1 and CRF2 receptor functions in the amygdala in pain-related synaptic facilitation and behavior. J Neurosci. 2008; 28:3861–3876. [PubMed: 18400885]
18. Gao X, Kim HK, Chung JM, Chung K. Reactive oxygen species (ROS) are involved in enhancement of NMDA-receptor phosphorylation in animal models of pain. Pain. 2007; 131:262–271. [PubMed: 17317010]
19. Gauriau C, Bernard J-F. Pain pathways and parabrachial circuits in the rat. Exp Physiol. 2002; 87:251–258. [PubMed: 11856971]
20. Gauriau C, Bernard J-F. A comparative reappraisal of projections from the superficial laminae of the dorsal horn in the rat: the forebrain. J Comp Neurol. 2004; 468:24–56. [PubMed: 14648689]
21. Goncalves L, Dickenson AH. Asymmetric time-dependent activation of right central amygdala neurones in rats with peripheral neuropathy and pregabalin modulation. Eur J Neurosci. 2012; 36:3204–3213. [PubMed: 22861166]
22. Greenwood-Van Meerveld B, Gibson M, Gunder W, Shepard J, Foreman R, Myers D. Stereotaxic delivery of corticosterone to the amygdala modulates colonic sensitivity in rats. Brain Res. 2001; 893:135–142. [PubMed: 11223001]
23. Han JS, Bird GC, Li W, Neugebauer V. Computerized analysis of audible and ultrasonic vocalizations of rats as a standardized measure of pain-related behavior. J Neurosci Meth. 2005; 141:261–269.
24. Han JS, Neugebauer V. Synaptic plasticity in the amygdala in a visceral pain model in rats. Neuroscience Letters. 2004; 361:254–257. [PubMed: 15135941]
25. Harrigan EA, Magnuson DJ, Thunstedt GM, Gray TS. Corticotropin releasing factor neurons are innervated by calcitonin gene-related peptide terminals in the rat central amygdaloid nucleus. Brain Res Bull. 1994; 33:529–534. [PubMed: 8186998]
26. Hidalgo C, Donoso P. Crosstalk between calcium and redox signaling: from molecular mechanisms to health implications. Antioxid Redox Signal. 2008; 10:1275–1312. [PubMed: 18377233]
27. Ji G, Fu Y, Adwanikar H, Neugebauer V. Non-pain-related CRF1 activation in the amygdala facilitates synaptic transmission and pain responses. Mol Pain. 2013; 9:2. [PubMed: 23410057]
28. Ji G, Neugebauer V. Hemispheric lateralization of pain processing by amygdala neurons. J Neurophysiol. 2009; 1102:2253–2264. [PubMed: 19625541]
29. Ji G, Neugebauer V. Reactive oxygen species are involved in group I mGluR-mediated facilitation of nociceptive processing in amygdala neurons. J Neurophysiol. 2010; 104:218–229. [PubMed: 20463194]
30. Ji G, Sun H, Fu Y, Li Z, Pais-Vieira M, Galhardo V, Neugebauer V. Cognitive impairment in pain through amygdala-driven prefrontal cortical deactivation. J Neurosci. 2010; 30:5451–5464. [PubMed: 20392966]
31. Johnson AC, Myers B, Lazovic J, Towner R, Greenwood-Van MB. Brain activation in response to visceral stimulation in rats with amygdala implants of corticosterone: an FMRI study. PLoS One. 2010; 5:e8573. [PubMed: 20052291]
32. Kato K, Clifford DB, Zorumski CF. Long-term potentiation during whole-cell recording in rat hippocampal slices. Neuroscience. 1993; 53:39–47. [PubMed: 8097020]
33. Keeble JE, Bodkin JV, Liang L, Wodarski R, Davies M, Fernandes ES, Coelho CD, Russell F, Graepel R, Muscara MN, Malcangio M, Brain SD. Hydrogen peroxide is a novel mediator of inflammatory hyperalgesia, acting via transient receptor potential vanilloid 1-dependent and independent mechanisms. Pain. 2009; 141:135–142. [PubMed: 19059721]
34. Khattab MM. TEMPOL, a membrane-permeable radical scavenger, attenuates peroxynitrite- and superoxide anion-enhanced carrageenan-induced paw edema and hyperalgesia: A key role for superoxide anion. European Journal of Pharmacology. 2006; 548:167–173. [PubMed: 16973155]

Author Manuscript Author Manuscript Author Manuscript Author Manuscript

35. Kim HK, Park SK, Zhou JL, Taglialatela G, Chung K, Coggeshall RE, Chung JM. Reactive oxygen species (ROS) play an important role in a rat model of neuropathic pain. Pain. 2004; 111:116–124. [PubMed: 15327815]
36. Kim HY, Wang J, Lu Y, Chung JM, Chung K. Superoxide signaling in pain is independent of nitric oxide signaling. Neurorep. 2009; 20:1424–1428.
37. King T, Vera-Portocarrero L, Gutierrez T, Vanderah TW, Dussor G, Lai J, Fields HL, Porreca F. Unmasking the tonic-aversive state in neuropathic pain. Nat Neurosci. 2009; 12:1364–1366. [PubMed: 19783992]
38. Kishida KT, Klann E. Sources and targets of reactive oxygen species in synaptic plasticity and memory. Antioxid Redox Signal. 2007; 9:233–244. [PubMed: 17115936]
39. Kulkarni B, Bentley DE, Elliott R, Julyan PJ, Boger E, Watson A, Boyle Y, El-Deredy W, Jones AK. Arthritic pain is processed in brain areas concerned with emotions and fear. Arthritis Rheum. 2007; 56:1345–1354. [PubMed: 17393440]
40. Labus JS, Gupta A, Coveleskie K, Tillisch K, Kilpatrick L, Jarcho J, Feier N, Bueller J, Stains J, Smith S, Suyenobu B, Naliboff B, Mayer EA. Sex differences in emotion-related cognitive processes in irritable bowel syndrome and healthy control subjects. Pain. 2013; 154:2088–2099. [PubMed: 23791896]
41. Laight DW, Andrews TJ, Haj-Yehia AI, Carrier MJ, Anggard EE. Microassay of superoxide anion scavenging activity in vitro. Environ Toxicol Pharmacol. 1997; 3:65–68. [PubMed: 21781760]
42. Lee I, Kim HK, Kim JH, Chung K, Chung JM. The role of reactive oxygen species in capsaicin-induced mechanical hyperalgesia and in the activities of dorsal horn neurons. Pain. 2007; 133:9–17. [PubMed: 17379413]
43. Lee KY, Chung K, Chung JM. Involvement of reactive oxygen species in long-term potentiation in the spinal cord dorsal horn. J Neurophysiol. 2010; 103:382–391. [PubMed: 19906875]
44. Li Z, Ji G, Neugebauer V. Mitochondrial reactive oxygen species are activated by mGluR5 through IP3 and activate ERK and PKA to increase excitability of amygdala neurons and pain behavior. J Neurosci. 2011; 31:1114–1127. [PubMed: 21248136]
45. Liu CC, Ohara S, Franaszczuk P, Zagzoog N, Gallagher M, Lenz FA. Painful stimuli evoke potentials recorded from the medial temporal lobe in humans. Neuroscience. 2010; 165:1402–1411. [PubMed: 19925853]
46. Maher P, Schubert D. Signaling by reactive oxygen species in the nervous system. Cell Mol Life Sci. 2000; 57:1287–1305. [PubMed: 11028919]
47. Mamdani F, Rollins B, Morgan L, Sequeira PA, Vawter MP. The somatic common deletion in mitochondrial DNA is decreased in schizophrenia. Schizophr Res. 2014 in press.
48. Masood A, Nadeem A, Mustafa SJ, O'Donnell JM. Reversal of oxidative stress-induced anxiety by inhibition of phosphodiesterase-2 in mice. J Pharmacol Exp Ther. 2008; 326:369–379. [PubMed: 18456873]
49. Massaad CA, Klann E. Reactive oxygen species in the regulation of synaptic plasticity and memory. Antioxid Redox Signal. 2011; 14:2013–2054. [PubMed: 20649473]
50. Medina G, Ji G, Gregoire S, Neugebauer V. Nasal application of neuropeptide S inhibits arthritis pain-related behaviors through an action in the amygdala. Mol Pain. 2014; 10:32. [PubMed: 24884567]
51. Miller MW, Sadeh N. Traumatic stress, oxidative stress and post-traumatic stress disorder: neurodegeneration and the accelerated-aging hypothesis. Mol Psychiatry. 2014; 19:1156–1162. [PubMed: 25245500]
52. Myers B, Greenwood-Van Meerveld B. Corticosteroid receptor-mediated mechanisms in the amygdala regulate anxiety and colonic sensitivity. Am J Physiol Gastrointest Liver Physiol. 2007; 292:G1622–G1629. [PubMed: 17347454]
53. Nakagawa T, Katsuya A, Tanimoto S, Yamamoto J, Yamauchi Y, Minami M, Satoh M. Differential patterns of c-fos mRNA expression in the amygdaloid nuclei induced by chemical somatic and visceral noxious stimuli in rats. Neuroscience Letters. 2003; 344:197–200. [PubMed: 12812839]

Author Manuscript Author Manuscript Author Manuscript Author Manuscript

54. Nakao A, Takahashi Y, Nagase M, Ikeda R, Kato F. Role of capsaicin-sensitive C-fiber afferents in neuropathic pain-induced synaptic potentiation in the nociceptive amygdala. Mol Pain. 2012; 8:51. [PubMed: 22776418]
55. Naliboff BD, Berman S, Chang L, Derbyshire SWG, Suyenobu B, Vogt BA, Mandelkern M, Mayer EA. Sex-related differences in IBS patients: central processing of visceral stimuli. Gastroenterology. 2003; 124:1738–1747. [PubMed: 12806606]
56. Neugebauer V, Galhardo V, Maione S, Mackey SC. Forebrain pain mechanisms. Brain Res Rev. 2009; 60:226–242. [PubMed: 19162070]
57. Neugebauer V, Han JS, Adwanikar H, Fu Y, Ji G. Techniques for assessing knee joint pain in arthritis. Mol Pain. 2007; 3:8–20. [PubMed: 17391515]
58. Neugebauer V, Li W, Bird GC, Han JS. The amygdala and persistent pain. Neuroscientist. 2004; 10:221–234. [PubMed: 15155061]
59. Paxinos, G.; Watson, C. The rat brain in stereotaxic coordinates. New York: Academic Press; 1998.
60. Pellmar TC. Peroxide alters neuronal excitability in the CA1 region of guinea-pig hippocampus in vitro. Neuroscience. 1987; 23:447–456. [PubMed: 3437974]
61. Pellmar TC, Gilman SC, Keyser DO, Lee KH, Lepinski DL, Livengood D, Myers LS Jr. Reactive oxygen species on neural transmission. Ann N Y Acad Sci. 1994; 738:121–129. [PubMed: 7832422]
62. Reddy PH, Reddy TP. Mitochondria as a therapeutic target for aging and neurodegenerative diseases. Curr Alzheimer Res. 2011; 8:393–409. [PubMed: 21470101]
63. Ren W, Kiritoshi T, Gregoire S, Ji G, Guerrini R, Calo G, Neugebauer V. Neuropeptide S: a novel regulator of pain-related amygdala plasticity and behaviors. J Neurophysiol. 2013; 110:1765–1781. [PubMed: 23883857]
64. Ren W, Neugebauer V. Pain-related increase of excitatory transmission and decrease of inhibitory transmission in the central nucleus of the amygdala are mediated by mGluR1. Mol Pain. 2010; 6:93–106. [PubMed: 21162731]
65. Rice, ME.; Avshalumov, MV.; Patel, JC. Hydrogen Peroxide as a Diffusible Messenger: Evidence from Voltammetric Studies of Dopamine Release in Brain Slices. In: Michael, AC.; Borland, LM., editors. Electrochemical Methods for Neuroscience. Vol. Chapter 11. Boca Raton, FL: CRC Press; 2007.
66. Schwaber JS, Sternini C, Brecha NC, Rogers WT, Card JP. Neurons containing calcitonin gene-related peptide in the parabrachial nucleus project to the central nucleus of the amygdala. J Comp Neurol. 1988; 270:416–426. [PubMed: 2836477]
67. Schwartz ES, Kim HY, Wang J, Lee I, Klann E, Chung JM, Chung K. Persistent pain is dependent on spinal mitochondrial antioxidant levels. J Neurosci. 2009; 29:159–168. [PubMed: 19129394]
68. Schwartz ES, Lee I, Chung K, Chung JM. Oxidative stress in the spinal cord is an important contributor in capsaicin-induced mechanical secondary hyperalgesia in mice. Pain. 2008; 138:514–524. [PubMed: 18375065]
69. Simons LE, Moulton EA, Linnman C, Carpino E, Becerra L, Borsook D. The human amygdala and pain: Evidence from neuroimaging. Hum Brain Mapp. 2014; 35:527–538. [PubMed: 23097300]
70. Tal M. A novel antioxidant alleviates heat hyperalgesia in rats with an experimental painful peripheral neuropathy. Neurorep. 1996; 7:1382–1384.
71. Tanimoto S, Nakagawa T, Yamauchi Y, Minami M, Satoh M. Differential contributions of the basolateral and central nuclei of the amygdala in the negative affective component of chemical somatic and visceral pains in rats. Eur J Neurosci. 2003; 18:2343–2350. [PubMed: 14622196]
72. Tillisch K, Mayer EA, Labus JS. Quantitative Meta-Analysis Identifies Brain Regions Activated During Rectal Distension in Irritable Bowel Syndrome. Gastroenterology. 2010; 140:91–100. [PubMed: 20696168]
73. Traub RJ, Silva E, Gebhart GF, Solodkin A. Noxious colorectal distension induced-c-Fos protein in limbic brain structures in the rat. Neurosci Letts. 1996; 215:165–168. [PubMed: 8899739]
74. Twining CM, Sloane EM, Milligan ED, Chacur M, Martin D, Poole S, Marsh H, Maier SF, Watkins LR. Peri-sciatic proinflammatory cytokines, reactive oxygen species, and complement induce mirror-image neuropathic pain in rats. Pain. 2004; 110:299–309. [PubMed: 15275780]

Author Manuscript Author Manuscript Author Manuscript Author Manuscript

75. Wang J, Cochran V, Abdi S, Chung JM, Chung K, Kim HK. Phenyl N-t-butylnitrone, a reactive oxygen species scavenger, reduces zymosan-induced visceral pain in rats. Neurosci Lett. 2008; 439:216–219. [PubMed: 18514415]

76. Watabe AM, Ochiai T, Nagase M, Takahashi Y, Sato M, Kato F. Synaptic potentiation in the nociceptive amygdala following fear learning in mice. Mol Brain. 2013; 6:11. [PubMed: 23452928]

77. Wilder-Smith CH, Schindler D, Lovblad K, Redmond SM, Nirkko A. Brain functional magnetic resonance imaging of rectal pain and activation of endogenous inhibitory mechanisms in irritable bowel syndrome patient subgroups and healthy controls. Gut. 2004; 53:1595–1601. [PubMed: 15479679]

78. Wilson CB, McLaughlin LD, Nair A, Ebenezer PJ, Dange R, Francis J. Inflammation and oxidative stress are elevated in the brain, blood, and adrenal glands during the progression of post-traumatic stress disorder in a predator exposure animal model. PLoS One. 2013; 8:e76146. [PubMed: 24130763]

Author Manuscript Author Manuscript Author Manuscript Author Manuscript

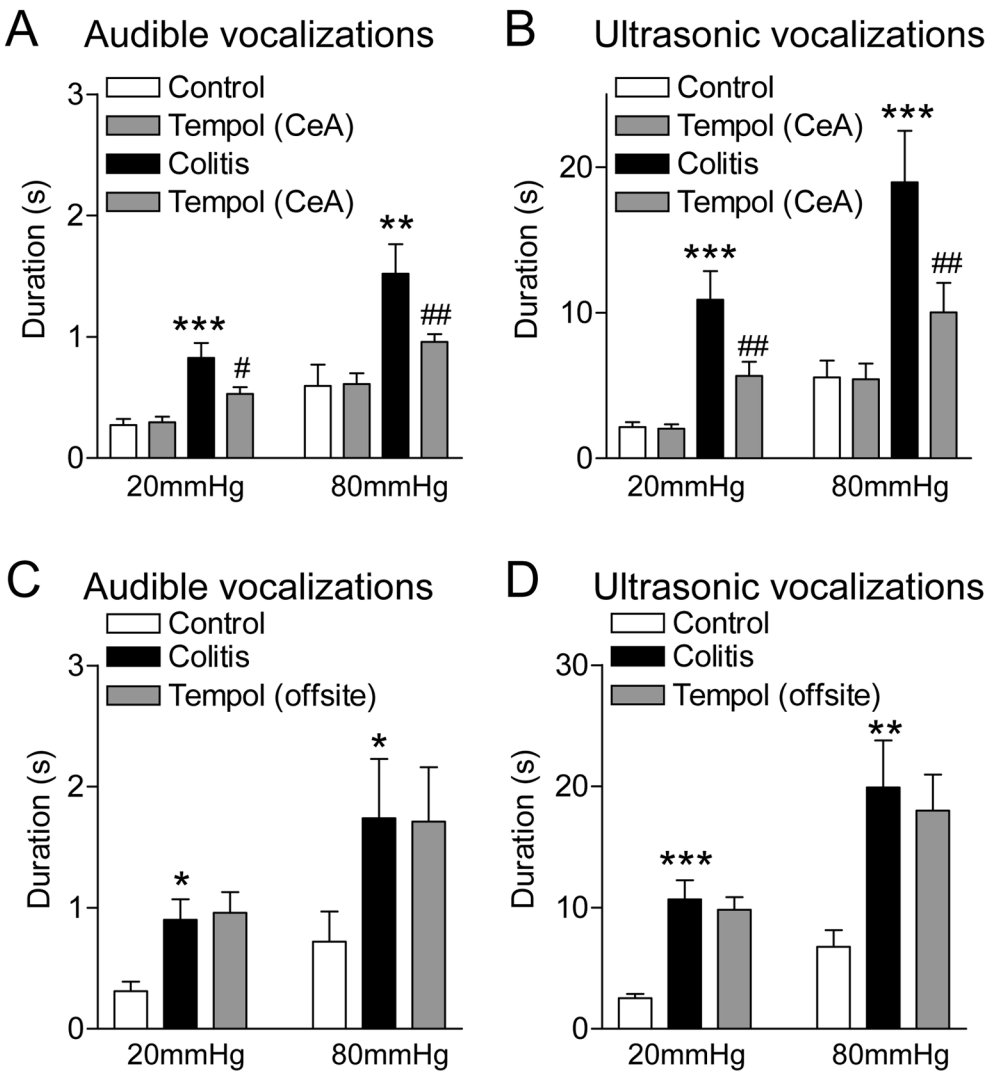

Figure 1. ROS scavenger (tempol) inhibits vocalizations in a visceral pain model

Bar histograms show the duration (mean ± SE) of audible (A,C) and ultrasonic (B,D) vocalizations evoked by brief (10 s) colorectal distension (CRD) with innocuous (20 mmHg) and noxious (80 mmHg) intraluminal pressure (see Methods). **A,B,** Stereotaxic application of a ROS scavenger (tempol, 100 mM, concentration in microdialysis probe, 15 min) into the amygdala (CeA) had no effect on vocalizations of normal rats ("control") but inhibited the increased vocalizations 5 h after intracolonic zymosan ("colitis") significantly (n = 5 rats). **C,D,** Off-site application of tempol into the adjacent striatum had no significant effect (n = 5 rats). *,**,*** $P < 0.05$-0.001 compared to normal (control); $^{\#,\#\#}$ $P < 0.05$, 0.01, compared to predrug baseline vocalizations measured in the presence of ACSF (vehicle control; see Methods), Bonferroni posttests following repeated-measures ANOVA.

Author Manuscript Author Manuscript Author Manuscript Author Manuscript

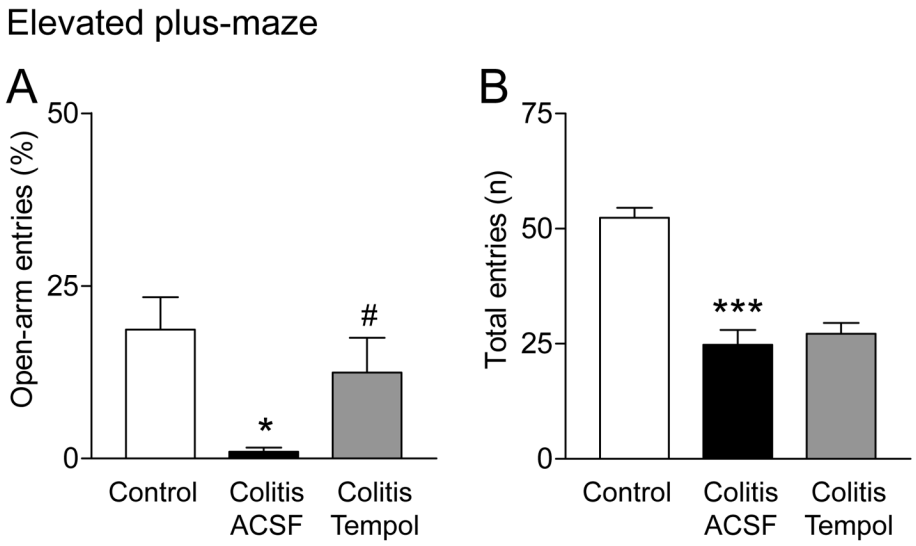

Figure 2. Tempol inhibits anxiety-like behavior but not locomotor activity in a visceral pain model

A, Bar histograms show the ratio of open-arm entries to the total number of entries (expressed as %) in the elevated plus-maze (EPM, mean ± SE) in three groups of rats. Sham controls (n = 5 rats). Rats with intracolonic zymosan ("colitis"; 5 h post-injection; n = 5) receiving stereotaxic application of ACSF (vehicle control) into the amygdala (CeA). Rats with intracolonic zymosan ("colitis", 5 h post-injection; n = 6) receiving stereotaxic application of tempol (100 mM, concentration in microdialysis probe, 15 min) into the CeA, which increased the open-arm preference significantly. **B,** Bar histograms show the total number (n) of entries into the open and closed arms of the EPM in the three groups of rats (same as in 2A) to determine any effects of tempol on locomotor activity. Tempol had no significant effect on locomotor activity. *,*** $P < 0.05, 0.001$, compared to sham controls; $^{\#}$ $P < 0.05$, compared to vehicle, Bonferroni posttests.

Author Manuscript Author Manuscript Author Manuscript Author Manuscript

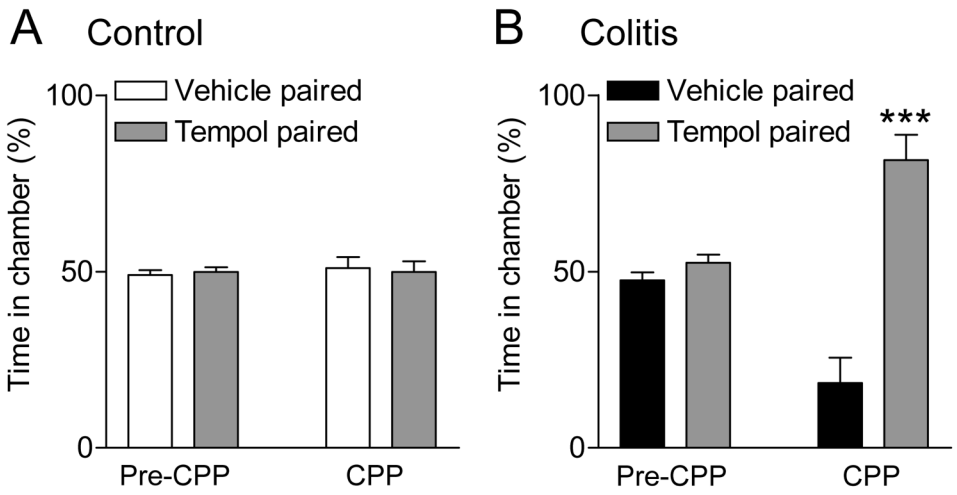

Figure 3. Tempol induces place preference in a visceral pain model

The conditioned place preference (CPP) test was performed in sham control rats (n = 7; **A**) and in rats with intracolonic zymosan (n = 6; **B**). Bar histograms show the ratio of time spent in each of two chambers of the place preference apparatus (mean ± SE expressed as %). There was no preference for one of the chambers before the pairing (pre-CPP). After stereotaxic application of ACSF (vehicle) into the CeA paired with one chamber for 30 min followed by stereotaxic application of tempol (100 mM, concentration in microdialysis probe, 15 min) paired with the opposite chamber for 30 min 4 h later, zymosan-injected animals ("colitis") preferred the chamber that was paired with tempol (**B**) whereas sham control rats did not show a preference (**A**). *** $P < 0.001$, time in tempol-paired chamber compared to vehicle-paired chamber, Bonferroni posttest.

Author Manuscript Author Manuscript Author Manuscript Author Manuscript

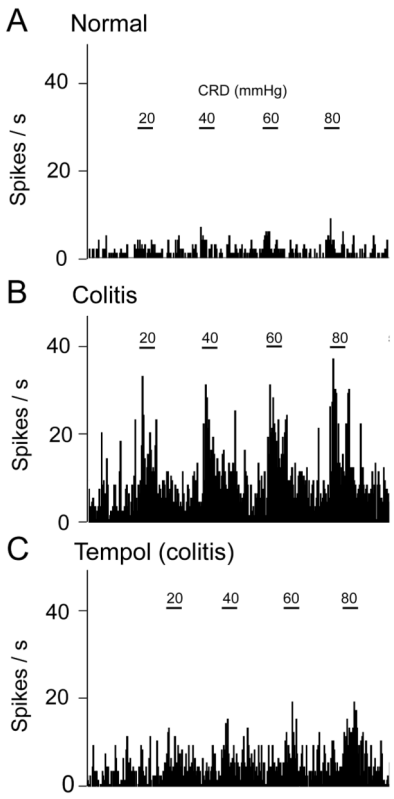

Figure 4. Tempol inhibits background and evoked activity of a CeA neuron in a visceral pain model

A, Responses of one CeA neuron to brief (10 s) graded CRD (innocuous, 20; moderate, 40; noxious, 60 and 80 mmHg) under normal conditions. **B,** The same neuron developed increased background and CRD-evoked activity 5 h after intracolonic zymosan ("colitis", visceral pain model). **C,** Stereotaxic application of tempol (100 mM, concentration in microdialysis probe; 15 min) decreased the activity. Peristimulus time histograms (bin width, 1 s) show number of action potentials (spikes) per second. Horizontal bars indicate CRD (10 s) and serve as scale bars.

Author Manuscript Author Manuscript Author Manuscript Author Manuscript

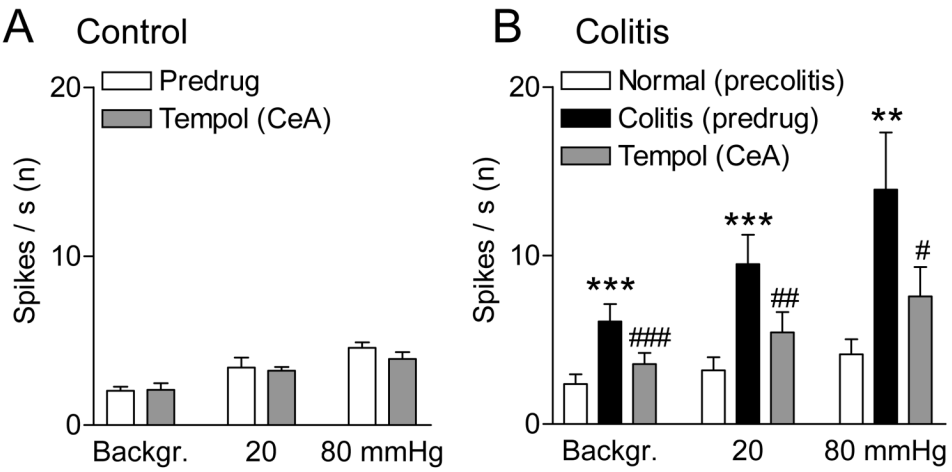

Figure 5. Summary of inhibitory effects of tempol on CeA neurons in a visceral pain model

A, Background and CRD-evoked activity in CeA neurons recorded in sham controls (rats with intracolonic saline). Stereotaxic application of tempol (100 mM, concentration in microdialysis probe, 15 min) into the CeA had no effect compared to predrug ACSF vehicle control (n = 5 neurons). **B,** Background and CRD-evoked activity increased significantly 5 h after intracolonic zymosan ("colitis"; n = 7 neurons). Intra-CeA tempol (100 mM, concentration in microdialysis probe, 15 min) inhibited activity of the same CeA neurons significantly compared to predrug ACSF control values. Bar histograms show spikes/s averaged across the sample of neurons. **,*** $P < 0.01, 0.001$ compared to normal; #,##,### $P < 0.05$-0.001, compared to predrug controls, Bonferroni posttests.

Author Manuscript Author Manuscript Author Manuscript Author Manuscript

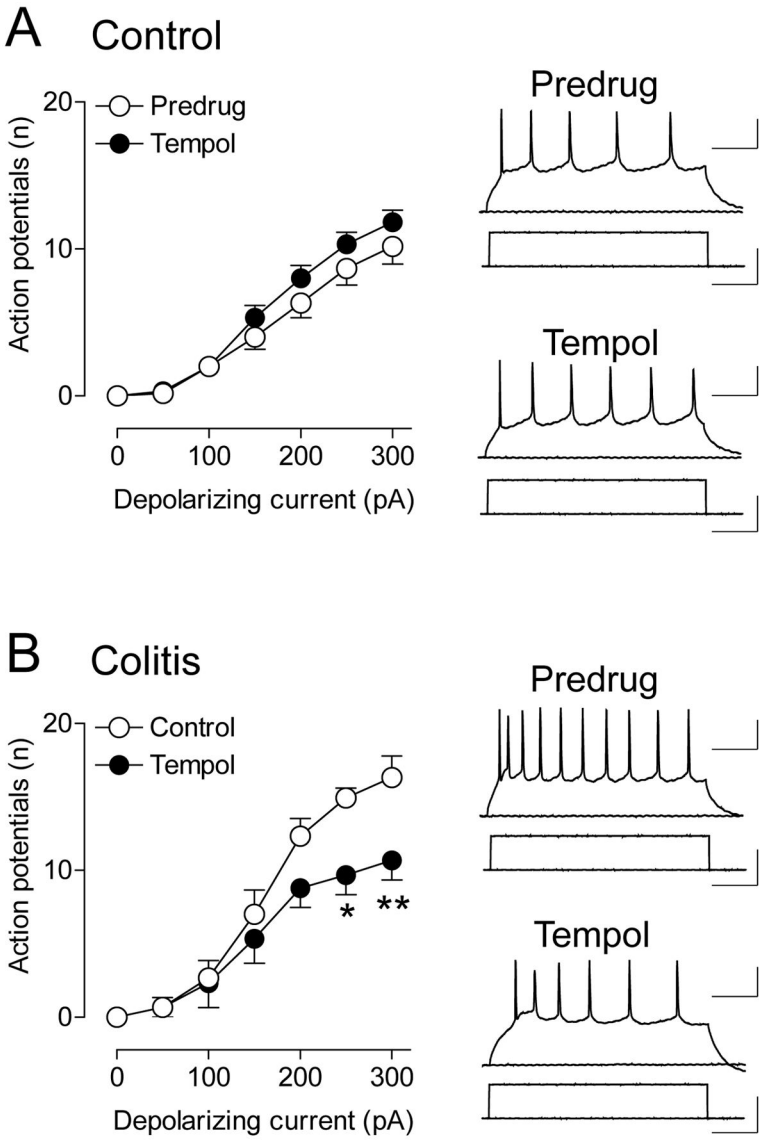

Figure 6. Tempol decreases excitability of CeA neurons in a visceral pain model

Whole-cell current-clamp recordings of action potentials generated in CeA neurons by intracellular (through the patch electrode) injections of depolarizing current pulses (500 ms) of increasing magnitude (in 100 pA steps) from a membrane potential of −60 mV. Graphs show input-output functions (frequency-current [F-I] relationships) averaged for the sample of neurons. Traces show action potential firing and depolarizing current steps. **A,** In brain slices from sham control rats treated with intracolonic saline, tempol (1 mM) had no effect on action potential firing (n = 5 neurons, $F_{1,56} = 5.42$, $P > 0.05$, main effect of drug, two-way ANOVA). **B,** In brain slices from rats with intracolonic zymosan (“colitis”; 5 h postinjection), tempol (1 mM) decreased action potential firing significantly (n = 6 neurons, $F_{1,70} = 13.66$, $P < 0.001$, main effect of drug, two-way ANOVA). Scale bars, 100 ms, 25 mV (current traces), 100 ms, 100 pA (voltage traces). *,** $P < 0.05,0.01$, Bonferroni posttests.

Author Manuscript Author Manuscript Author Manuscript Author Manuscript

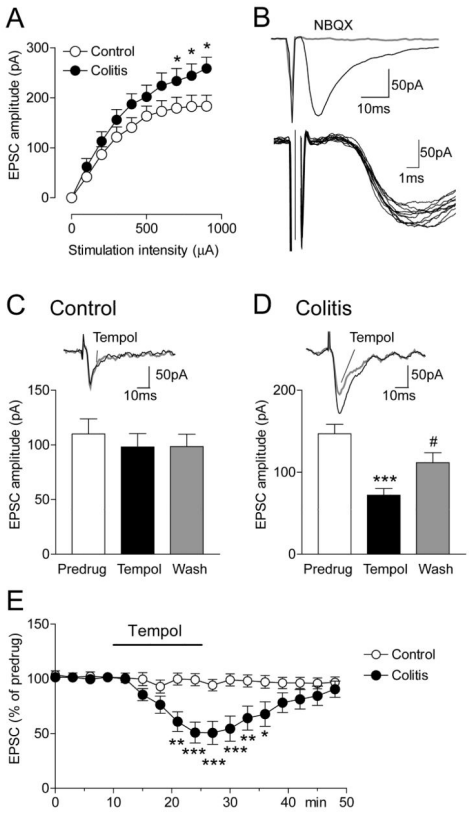

Figure 7. Tempol inhibits excitatory synaptic transmission in CeA neurons in a visceral pain model

Whole-cell voltage-clamp recordings of monosynaptic EPSCs evoked in CeA neurons by stimulation of presumed afferents from the parabrachial area (see Methods and Discussion) were measured in slices from sham controls and from rats with intracolonic zymosan ("colitis"; 5 h postinjection). **A,** Input-output functions of EPSCs were significantly increased in slices from zymosan-treated rats (n = 13 neurons) compared to controls (n = 10 neurons; $F_{1,210} = 19.95$, $P < 0.001$, main effect of drug, two-way ANOVA. **B,** Individual traces show that EPSCs were monosynaptic with constant latency and kinetics. EPSCs were blocked by a non-NMDA receptor antagonist (NBQX, 10 μM). **C,** Tempol (1 mM) had no effect on baseline transmission in slices from sham controls (n = 5 neurons). **D,** Tempol inhibited EPSCs in slices from zymosan-treated rats (n = 9 neurons; $P < 0.001$, Bonferroni posttest). Effects were reversible upon washout (20 min). **C,D,** Bar histograms show means ± SEM. *** $P < 0.001$, compared to predrug; $^{\#}$ $P < 0.05$, compared to drug, Bonferroni posttests. **E,** Time course of the effects of tempol in slices from controls (n = 5 neurons) and from rats with colitis (n = 5). Symbols show means ± SEM. *,**,*** $P < 0.05$, 0.01, 0.001, colitis compared to control, Bonferroni posttests.

Author Manuscript Author Manuscript Author Manuscript Author Manuscript

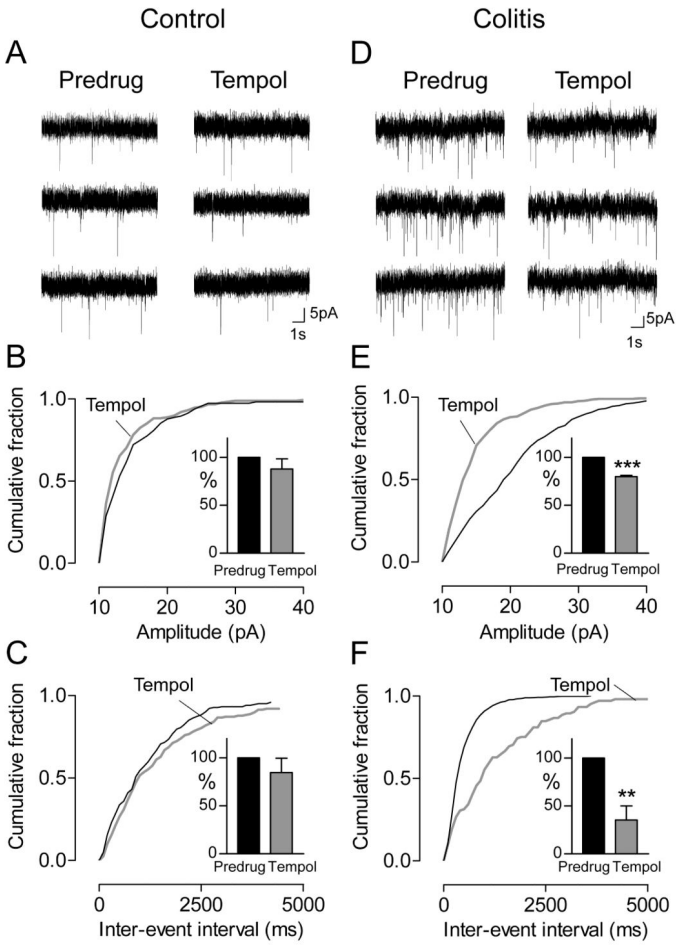

Figure 8. Tempol inhibits amplitude and frequency of miniature EPSCs in a visceral pain model

Whole cell voltage-clamp recordings of CeA neurons in brain slices from sham controls **(A–C)** and rats with intracolonic zymosan ("colitis"; **D–F**). **A,D,** Current traces of mEPSCs (in TTX, 1 μM) in individual CeA neurons before (Predrug) and during tempol (1 mM). **B–F,** Cumulative distribution analysis of mEPSC amplitude **(B,E)** and frequency **(C,F)** measured over periods of 5 min. Graphs show cumulative distributions of mEPSC amplitude and frequency in individual neurons. Bar histograms show mean mEPSC amplitude and frequency in the sample of neurons normalized to predrug values (mean ± SEM). **B,C,** Tempol (1 mM) had no significant effect in controls (n = 5 neurons). **E,** Tempol shifted mEPSC amplitude distribution towards smaller values ($P < 0.05$, Kolmogorov-Smirnov test, individual example) and decreased mean mEPSC amplitude significantly (n = 6 neurons; $P < 0.001$, paired t-test). **F,** Tempol caused a shift towards larger inter-event intervals ($P < 0.05$, Kolmogorov-Smirnov test, individual example) hence decreasing mean mEPSC frequency significantly (n = 6 neurons; $P < 0.01$, paired t-test). **,*** $P < 0.01$, 0.001, compared to predrug (paired t-test).

Author Manuscript Author Manuscript Author Manuscript Author Manuscript

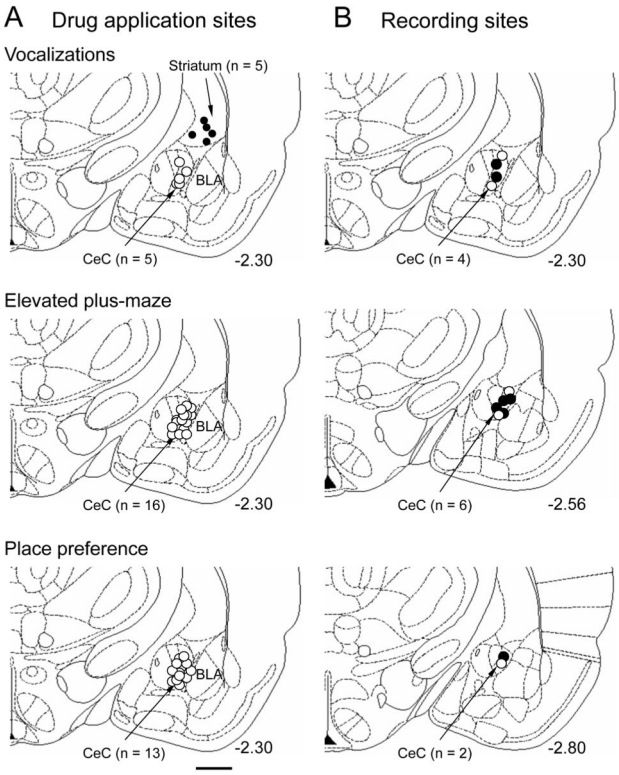

Figure 9. Histologically verified drug application and recording sites

A, Positions of the tips of the microdialysis probes in experiments measuring vocalizations (see Fig. 1, n = 10 animals), anxiety-like behavior (see Fig. 2, n = 16 animals) and place preference (see Fig. 3, n = 13 animals). Off-site controls in the striatum are indicated by filled symbols. **B,** Positions of the recording electrodes in the electrophysiology experiments in anesthetized animals (Figs. 4 and 5, n = 12 neurons). Open circles, sham controls; filled circles, zymosan model. **A,B,** Boundaries of different amygdala nuclei are easily identified under the microscope. CeC, central nucleus of the amygdala, capsular division; BLA, basolateral amygdala. Calibration bar, 1 mm. Numbers indicate distance from bregma.

Author Manuscript Author Manuscript Author Manuscript Author Manuscript

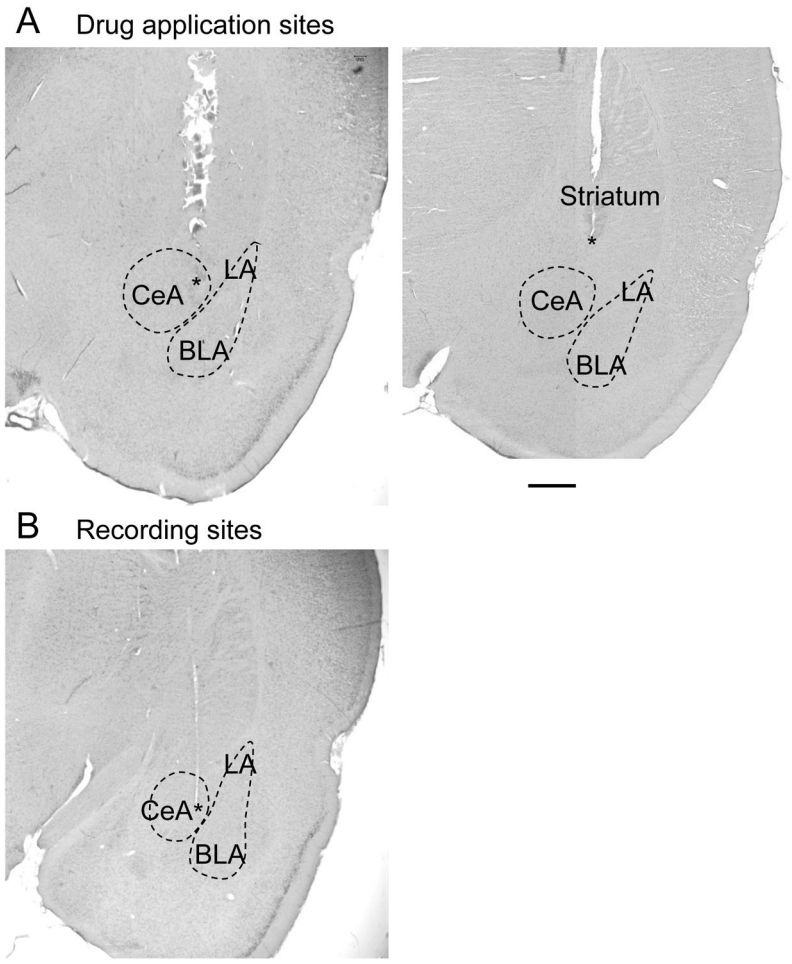

Figure 10. Histologic images of drug application and recording sites

A, Individual examples of histologically verified positions of microdialysis probes in the central nucleus of the amygdala (left) and striatum (placement control, right). Asterisks denote position of the tip of the microdialysis fiber which protruded the shaft of the probe by 1 mm. Note that the shaft left a larger lesion than the fiber. Removal of the probe and processing of the tissue likely increased the size of the lesion. **B,** Histologically verified position of the recording electrode in the capsular division of the central nucleus. Asterisk denotes position of the electrode tip. CeA, central nucleus of the amygdala; LA, BLA, lateral and basolateral amygdala. Calibration bar, 1 mm.